

TIDAL COMPUTATION IN THE GULF OF CALIFORNIA I

NICOLAS GRIJALVA*

RESUMEN

El fenómeno de mareas que ocurre en el Golfo de California tiene gran importancia debido a las grandes amplitudes de la parte norte. Además la generación de ondas internas y la deflexión gravitacional del fondo, hacen el estudio de importancia. La inducción de la marea puede ser tomada en cuenta por dos mecanismos fundamentalmente diferentes: a) las fuerzas generadoras de mareas y b) la oscilación periférica con el Océano Pacífico.

El método descrito puede tomar en consideración ambos mecanismos y no requiere despreciar métodos no lineales. En este trabajo se calcula la marea M_2 para todo el Golfo como el primer ensayo. Los resultados se comparan con observaciones.

ABSTRACT

The tidal phenomena that takes place in the Gulf of California is of a great importance due to the big amplitudes in the northern part. Besides, the coupling with internal modes and the gravitational deflection of the bottom make the tidal study of importance. The tidal drive can be taken into account by two fundamentally different mechanisms; a) the tide generating forces and b) the peripheral oscillation with the Pacific Ocean.

The method described here can take into account both mechanisms and also, it does not require neglecting non-linear terms. In this paper the M_2 tidal constituent is computed for the Gulf as the first trial of the method. The results are compared with observed data.

* *Instituto de Geofísica, UNAM, Instituto Nacional de Energía Nuclear, México, Scripps Institution of Oceanography UCSD, USA.*

I INTRODUCTION

The Gulf of California is an almost closed region with accurately known topography, and since the tidal energy which enters through its open end can be determined with great approximation with modern instrumentation, (J. Filoux, 1970, 1971) it is possible, in principle, to compute the configuration of the tide within the Gulf provided one knows the dynamical interaction of the tide with its borders. Therefore, the Gulf can be used as a geophysical laboratory to study problems related to ocean tides.

The tidal phenomena that can be studied by the knowledge of the tide are of subtle nature which are not only caused by the tidal forces, but also have an influence on its own propagation. Among them one can count the coupling of the tide with internal modes which occurs in basins deep enough as the Gulf and where the water is stratified. It is also important the self gravitational deflection of the sea bottom due to the loading of the Gulf. Therefore, the use of the Gulf in this sense requires accurate methods of calculation of the tidal propagation. It is the purpose of this paper to examine one method of such computations.

The method used here allows the use of two fundamentally different mechanism of tidal driving; 1) the gravitational forces acting in the entire Gulf and 2) the peripheral co-oscillation with the Pacific Ocean along the open boundary.

It permits the inclusion of some non-linear terms which enables us to detect overtones which are, in some way, measure of tidal energy dissipation.

II THE METHOD

The hydrodynamic differential equations can be written in the following way:

a) The equations of motion:

$$\frac{du}{dt} + \frac{1}{\rho} R^{(x)} - fu + g \frac{\partial \zeta}{\partial x} = \frac{1}{\rho} F^{(x)} \quad (1-a)$$

$$\frac{dv}{dt} + \frac{1}{\rho} R^{(y)} + fu + g \frac{\partial \zeta}{\partial y} = \frac{1}{\rho} F^{(y)} \quad (1-b)$$

b) The equation of continuity:

$$\frac{\partial u}{\partial x} + \frac{\partial v}{\partial y} + \frac{\partial w}{\partial z} = 0 \quad (1-c)$$

x, y and z are the cartesian coordinates in the eastern, northern and zenithal directions respectively.

u, v and w are the components of the velocity in the x, y and z directions respectively.

$R^{(x)}$, $R^{(y)}$ are the components of the friction in the x and y directions respectively.

$f = 2 \omega \sin \varphi$ is the Coriolis parameter, ω is the angular velocity of the earth and φ is the latitude of the point.

g is the earth gravitational acceleration.

ζ is the deviation of the sea level from an undisturbed ocean.

ρ is the density.

$F^{(x)}$ and $F^{(y)}$ are the component of the tide generating forces in the x and y directions.

$$\frac{du}{dt} = \frac{\partial u}{\partial t} + u \frac{\partial u}{\partial x} + v \frac{\partial u}{\partial y}$$

$$\frac{dv}{dt} = \frac{\partial v}{\partial t} + u \frac{\partial v}{\partial x} + v \frac{\partial v}{\partial y}$$

The following assumption is made with respect to the friction terms, (S. H. Lamb, 1935)

$$\frac{1}{\rho} R^{(x)} = Ah \nabla^2 u + A v \frac{\partial^2 u}{\partial z^2}$$

$$\frac{1}{\rho} R^{(y)} = Ah \nabla^2 v + A u \frac{\partial^2 v}{\partial z^2}$$

Where A is the eddy viscosity coefficient.

The equations (1) are now integrated from the bottom $z = -h(x, y)$ to the sea level $z = \zeta(x, y, t)$. The integration is explained by Brettschneider, (1967) and Grijalva (1971). The following relations are considered valid:

$$\frac{1}{H} \int_{-h}^{\zeta} \frac{\partial u}{\partial t} dz = \frac{\partial}{\partial t} \left(\frac{1}{H} \int_{-h}^{\zeta} u dz \right) = \frac{\partial U}{\partial t}$$

$$\frac{1}{H} \int_{-h}^{\zeta} \frac{\partial u}{\partial x} dz = \frac{\partial}{\partial x} \left(\frac{1}{H} \int_{-h}^{\zeta} u dz \right) = \frac{\partial U}{\partial x}$$

$$\frac{1}{H} \int_{-h}^{\zeta} \frac{\partial u}{\partial y} dz = \frac{\partial}{\partial y} \left(\frac{1}{H} \int_{-h}^{\zeta} u dz \right) = \frac{\partial U}{\partial y}$$

and similar expressions for v. Then:

$$\frac{1}{H} \int_{-h}^{\zeta} \left(u \frac{\partial u}{\partial x} + v \frac{\partial u}{\partial y} \right) dz = U \frac{\partial U}{\partial x} + V \frac{\partial U}{\partial y}$$

$$\frac{1}{H} \int_{-h}^{\zeta} \left(u \frac{\partial v}{\partial x} + v \frac{\partial v}{\partial y} \right) dz = U \frac{\partial V}{\partial x} + V \frac{\partial V}{\partial y}$$

$$\frac{1}{H} \int_{-h}^{\zeta} Ah \nabla^2 u dz = Ah \nabla^2 U$$

$$\frac{1}{H} \int_{-h}^{\zeta} Ah \nabla^2 v dz = Ah \nabla^2 V$$

where $H = h + \zeta$ is the instantaneous depth and

$$U = \frac{1}{H} \int_{-h}^{\zeta} u \, dz \quad V = \frac{1}{H} \int_{-h}^{\zeta} v \, dz$$

Equations 1 become: (2 -a)

$$\frac{\partial U}{\partial t} + U \frac{\partial U}{\partial x} + V \frac{\partial U}{\partial y} + \frac{1}{H} \int_{-h}^{\zeta} A_v \frac{\partial^2 u}{\partial z^2} dz + Ah \nabla^2 U - fV + g \frac{\partial \zeta}{\partial x} = F^{(x)}$$

$$\frac{\partial V}{\partial t} + U \frac{\partial V}{\partial x} + V \frac{\partial V}{\partial y} + \frac{1}{H} \int_{-h}^{\zeta} A_v \frac{\partial^2 v}{\partial z^2} dz + Ah \nabla^2 V + fU + g \frac{\partial \zeta}{\partial y} = F^{(y)}$$

$$\frac{\partial \zeta}{\partial t} + \frac{\partial}{\partial x} (HU) + \frac{\partial}{\partial y} (HV) = 0 \quad (2 -c)$$

$$\left[A_v \frac{\partial u}{\partial z} \right]_{-h}^{\zeta}, \quad \left[A_v \frac{\partial v}{\partial z} \right]_{-h}^{\zeta}$$

are the tangential frictional forces on the surface and the bottom of the sea. The friction term on the bottom is taken proportional to the mean velocity square:

$$\left[A_v \frac{\partial u}{\partial z} \right]_{z = -h} = C_D \sqrt{U^2 + V^2} \quad U = R H U$$

$$\left[A_v \frac{\partial v}{\partial z} \right]_{z = -h} = C_D \sqrt{U^2 + V^2} \quad V = R H V$$

C_D is a dimensionless coefficient, whose range of values, according to estimates of several authors (Taylor, 1919), (Grace, 1936); (Bowden and Fairbairn, 1952),

$$\text{is } 21.3 \times 10^{-3} \cong C_D \cong 0.28 \times 10^{-3}$$

The value of the friction on the surface is not taken into account because this paper deals only with tides.

Equations (2) now become:

$$\frac{\partial U}{\partial t} + U \frac{\partial U}{\partial x} + V \frac{\partial U}{\partial y} + RU - A_h \nabla^2 U - fV + g \frac{\partial \zeta}{\partial x} = F(x) \quad (3-a)$$

$$\frac{\partial V}{\partial t} + U \frac{\partial V}{\partial x} + V \frac{\partial V}{\partial y} + RV - A_h \nabla^2 V + fU + g \frac{\partial \zeta}{\partial y} = F(y) \quad (3-b)$$

$$\frac{\partial \zeta}{\partial t} + \frac{\partial}{\partial x} (HU) + \frac{\partial}{\partial y} (HV) = 0 \quad (3-c)$$

To solve these equations the following boundary values will be used:

- 1) The component of the velocity normal to the coast is zero.
- 2) Along the boundary that lies on the open sea, the values of ζ are known at all times. If the viscosity terms were taken into account, another boundary condition is needed. Furthermore, the values of the derivative of the velocity normal the border are the set equal to zero.

The first boundary condition 1) (Dirichlet condition) does not yield a description of the physical phenomenon. It would be more appropriate to set, as boundary condition, the amount of energy dissipated along the coast. This amount is not yet known and therefore could not be used. The condition 1) used can be regarded as an approximation to the physical phenomenon.

III THE M_2 TIDE IN THE GULF OF CALIFORNIA

3.1 PRESENTATION

The first computations carried out in the Gulf were the corresponding to the M_2 tidal constituent. In the computations the advective terms and the tidal generating forces will not be taken into account. Therefore, equations (3-a), (3-b) and (3-c) become:

$$\frac{\partial U}{\partial t} + RU - fV + g \frac{\partial \zeta}{\partial x} = A_h \nabla^2 U \quad (4-a)$$

$$\frac{\partial V}{\partial t} + RV + fU + g \frac{\partial \zeta}{\partial y} = Ah \nabla^2 V \quad (4-b)$$

$$\frac{\partial \zeta}{\partial t} + \frac{\partial}{\partial x} (HU) + \frac{\partial}{\partial y} (HV) = 0 \quad (4-c)$$

The boundary conditions remain the same.

Equations 4 will be transformed into finite differences equations which are related to the grid net shown in figure 1.

One can distinguish three pivotal points:

- x where the velocity U is computed
- . where the velocity V is computed
- + where the sea level is computed.

Following this pattern equations 4 become:

$$u_{(I,J)}^{(t+\Delta t)} = (1 - Q_{(I,J)}^{x(t)}) \tilde{u}_{(I,J)}^{(t)} + 2\Delta t \cdot f \cdot \tilde{v}_{(I,J)}^{(t)} - \frac{\Delta t}{I} \cdot g (\zeta_{(I+1,J)}^{(t+\Delta t)} - \zeta_{(I-1,J)}^{(t+\Delta t)}) + 2\Delta t \cdot F_{(I,J)}^{x(t)}$$

$$v_{(I,J)}^{(t+\Delta t)} = (1 - Q_{(I,J)}^{y(t)}) \tilde{v}_{(I,J)}^{(t)} - 2\Delta t \cdot f \cdot u_{(I,J)}^{(t)} - \frac{\Delta t}{I} \cdot g (\zeta_{(I,J+1)}^{(t+\Delta t)} - \zeta_{(I,J-1)}^{(t+\Delta t)}) + 2\Delta t \cdot F_{(I,J)}^{y(t)}$$

$$\zeta_{(I,J)}^{(t+\Delta t)} = \zeta_{(I,J)}^{(t-\Delta t)} - \frac{\Delta t}{I} \left(H_{u(I+1,J)}^{(t-\Delta t)} u_{(I+1,J)}^{(t)} - H_{u(I-1,J)}^{(t-\Delta t)} u_{(I-1,J)}^{(t)} + H_{v(I,J-1)}^{(t-\Delta t)} v_{(I,J-1)}^{(t)} - H_{v(I,J+1)}^{(t-\Delta t)} v_{(I,J+1)}^{(t)} \right)$$

$$H_{u(I,J)}^{(t-\Delta t)} = h_{u(I,J)} + \frac{1}{2} (\zeta_{(I+1,J)}^{(t-\Delta t)} + \zeta_{(I-1,J)}^{(t-\Delta t)})$$

$$H_{v(I,J)}^{(t-\Delta t)} = h_{v(I,J)} + \frac{1}{2} (\zeta_{(I,J-1)}^{(t-\Delta t)} + \zeta_{(I,J+1)}^{(t-\Delta t)})$$

$$Q_{(I,J)}^{x(t)} = 2c_b \Delta t \left[\left(\mathbf{u}_{(I,J)}^{(t)} \right)^2 + \left(\mathbf{v}_{(I,J)}^{*(t)} \right)^2 \right]^{1/2} \left(H_{\mathbf{u}_{(I,J)}}^{(t+\Delta t)} \right)^{-1}$$

$$Q_{(I,J)}^{y(t)} = 2c_b \Delta t \left[\left(\mathbf{u}_{(I,J)}^{*(t)} \right)^2 + \left(\mathbf{v}_{(I,J)}^{(t)} \right)^2 \right]^{1/2} \left(H_{\mathbf{v}_{(I,J)}}^{(t+\Delta t)} \right)^{-1}$$

$$\mathbf{u}_{(I,J)}^{*(t)} = \frac{1}{4} \left(\mathbf{u}_{(I+1,J+1)}^{(t)} + \mathbf{u}_{(I+1,J-1)}^{(t)} + \mathbf{u}_{(I-1,J-1)}^{(t)} + \mathbf{u}_{(I-1,J+1)}^{(t)} \right)$$

$$\mathbf{v}_{(I,J)}^{*(t)} = \frac{1}{4} \left(\mathbf{v}_{(I+1,J+1)}^{(t)} + \mathbf{v}_{(I+1,J-1)}^{(t)} + \mathbf{v}_{(I-1,J-1)}^{(t)} + \mathbf{v}_{(I-1,J+1)}^{(t)} \right)$$

$$\tilde{\mathbf{u}}_{(I,J)}^{(t)} = \alpha \mathbf{u}_{(I,J)}^{(t)} + \frac{1-\alpha}{4} \left(\mathbf{u}_{(I+2,J)}^{(t)} + \mathbf{u}_{(I-2,J)}^{(t)} + \mathbf{u}_{(I,J+2)}^{(t)} + \mathbf{u}_{(I,J-2)}^{(t)} \right)$$

$$\tilde{\mathbf{v}}_{(I,J)}^{(t)} = \alpha \mathbf{v}_{(I,J)}^{(t)} + \frac{1-\alpha}{4} \left(\mathbf{v}_{(I+2,J)}^{(t)} + \mathbf{v}_{(I-2,J)}^{(t)} + \mathbf{v}_{(I,J+2)}^{(t)} + \mathbf{v}_{(I,J-2)}^{(t)} \right)$$

$$\alpha = 1 - 4 \left(\frac{A_n \Delta t}{l^2} \right)$$

3.2 STABILITY OF THE NUMERICAL COMPUTATIONS:

A necessary condition for the stability of the computations is the Courant, Friedrich-Lewy condition:

$$\Delta t < \frac{\Delta x \quad \Delta y}{\sqrt{gh_m [(\Delta x)^2 + (\Delta y)^2]}}$$

In the present paper $\Delta x = \Delta y$ then (7) becomes:

$$\Delta t < \frac{L}{\sqrt{gh_m}}$$

$L = \Delta x = \Delta y$, h_m is the maximum depth.

This condition is valid for linear systems but as the system here is quasilinear it is possible to use it. This has been proved in many computations.

3.3 THE NUMERICAL COMPUTATIONS

The computation grid net

The Gulf of California was covered by a grid net as shown in Fig. 1, the distance between two U, V or ζ points was constant 7000 m. The net consisted of 1387 U points and the same amount for V and ζ points giving a total of 4161 computing points. The boundaries followed the coastline along Baja California, Sonora and Sinaloa and an artificial boundary was set from Punta Arenas to Lucernilla. The dimensions of the model are shown in Fig. 2.

Depths

The depths were averaged around each U and V points from the charts published by the U. S. Navy Surveys Nrs. H0620, 621 and 622.

Boundary conditions

The boundary conditions along the coast were that the velocity component normal to the coast is set zero. Along the artificial boundary from Punta Arena to Lucernilla, (see Fig. 2); the values for ζ were prescribed:

$$\zeta = A \cos (\sigma t - \mathcal{H}) = \zeta_1 \cos \sigma t + \zeta_2 \sin \sigma t$$

The values for A and \mathcal{H} were interpolated linearly from observations in La Paz, Topolobampo and Mazatlán. For Punta Arenas the values were A = 0.29 m and $\mathcal{H} = 276^\circ$; for Lucernilla A = 0.37 m and $\mathcal{H} = 286^\circ$ (\mathcal{H} is referred to meridian 105 West of Greenwich).

Initial conditions

At the beginning of the computation the values of U , V , and ζ were set equal to zero, or in other words, the sea was at rest. Then the values along the southern boundary were increased from zero to their real values. Stability was reached after 5 periods, (Grijalva, 1971).

Constant values used for the computation

- a) The Coriolis parameter $f = 2 \omega \sin \varphi$ was computed for every point. The angular velocity of the earth was: $\omega = 72.92 \times 10^{-6} \text{ sec}^{-1}$ (sidereal time)
- b) The earth gravitational acceleration
 $g = 9.81 \text{ m/sec}^2$
- c) The pivotal distance $2L = 14000 \text{ m}$
- d) Timestep $2\Delta t = 57 \text{ sec}$

The maximum depth in the Gulf is 2800 m, the Courant, Friedrich, Lewy criterium was fulfilled

$$2\Delta t = 57 < \frac{2L}{\sqrt{2gh_m}} = 59.731 \text{ sec}$$

- e) The drag coefficient was taken as follows:
In the first computation, it was given the value
 $C_D = 0.003$, in the second the value was
 $C_D = 0.0045$

3.4 THE COMPUTER PROGRAM

The computations were carried out in a CDC 3600 Electronic Computer in the University of California, San Diego. Three computations were completed.

a) All the values were taken in account as described in 3.3, the drag coefficient was = 0.003

b) All the values were taken in account as described in 3.3, but the drag coefficient was = 0.0045.

c) The new drag coefficient = 0.0045 was used but the amplitudes in the opening, prescribed as boundary values, were reduced in 20%. The programs were written in FORTRAN 63.

It took the computer five tidal periods to establish the regime. After this, phases and amplitudes were printed for every 14 time steps.

3.5 RESULTS

As the computations were carried out by a time stepping technique it was easy to take the values of the sea level and the water velocities at a given time, then taking the values at a closed period ($t = T, 2T, 3T \dots .5T$) and a quarter of a period later, phases and amplitudes were computed. The results are then shown as cotidal and corange lines and also lines showing lines of equal values of ζ , and ζ_2 values. The process of the tide is shown in five points, and the currents are shown in five selected points during a period.

3.5a Propagation of the tide

In Fig. 3 it is seen the amplification of the tide in five different points (see Fig. 4). Point E and point D lie relatively near the open boundary. Here the tidal curve begins to show in the first quarter of a period. The amplitudes are small; in point E is near 30 cm as in the boundary. Points C, B and A lie north of the islands. Here the tidal curve begins to be noticed only in the second quarter of the first period in points C and B and in the thirrh quarter of a period in point A. The amplitudes in these three points are remarkably bigger than in the first two. In points A, B and C, the regime has not been

completely established. It is possible to observe that north of the islands the amplitudes grow very rapidly.

3.5.b Phases and amplitudes

Figs. 5, 6 and show the amplitude and phases computed for the three computations. In all figures some features are similar, and only details are different. Both the amplitudes and the phases show the characteristics of a Kelvin wave. The boundary conditions were such that simulate such a wave in the open boundary. This wave propagates inside of the Gulf first decreasing in amplitude and then north of the islands the amplitude grows from 50 cm to some 400 cm. In the southern part the amplitudes decrease down to 5 cm but an aphidromic point is not clearly shown. Around the islands, the amplitudes grow rapidly up to the northern part where the water piles up due both to the shallow areas and also to resonance effect. See Krummel (1911). This effect can be noticed also in the phases. The phase delay between the entrance and the northern top reaches some 180° .

The phases also show the Kelvin wave at the southern boundary, this picture is totally changed in the region of the islands and the northern part where due to the bottom topography, the cotidal lines are altered. Figure 6 shows similar characteristics as Fig. 5; the influence of the friction seems to be more important along the edges and in shallow areas as the northern part. Here the amplitudes do not grow as big, but only reach 360 cm. The change in phases is small and can hardly be noticed, also here the phase delay remains of 180° . The main changes have occurred here, as expected in shallow areas and along the edges. Fig. 7 shows the results of the third computation. The amplitudes are now smaller than before. A reduction of 20% is expected, but due to the non-linear terms taken in account the reduction is of 25% in some places and of 14.5% in other as, for instance, in Puerto Peñasco. The effect of the non-linearty can also be seen in the phases, as usual, along the coast and in the shallow areas north of the islands. The phase delay is again of 180° , see Handershot and Speranza (1971). Fig. 8 shows the values of ζ , and ζ_2 (See

3.3): here ζ_1 are the values of the sea level at a close period and ζ_2 are the values of the sea level a quarter of a period later. The values of ζ_1 show a picture of a wave entering the Gulf with a wave front perpendicular to the Gulf axis and propagating in this direction from -20 cm to 280 in the north. For ζ_2 the picture is completely changed. There is first an increase of values up to 67 cm and in the very top the values are negative. This agrees with the phases where it is shown that high water occurs first in the northern Sonora coast than in the Baja California side. This is to be expected due to the bottom topography.

3.5.c Tidal currents

Currents were plotted every 14 time steps in points A, B, C, D and E, the results are shown in Fig. 9. The currents are almost all of the alternating type, see Grijalva (1964), in point A, the biggest values are shown, almost a knot in each direction. Here the tidal ellipse turns clock wise. Point B shows smaller values of about 0.25 cm/sec in each direction. The currents are almost completely alternating, but it is still possible to see that it rotates in the clock wise direction. The currents in point C are stronger than those in point B, but one cannot see in which direction they rotate, they are completely alternating.

Points D and E are small currents of some 15 cm in value point D the ellipse rotate in the clock wise direction but in point E the currents rotate in the counter clock wise direction. Point E lies in very deep water and points A, B, C and D lie in relatively shallow water, specially point A, and the sense in which they rotate is a consequence of the passing Kelvin wave, the Coriolis parameter and the depth of the point. (Larsen, 1966), (Isaacs et al, 1966).

3.5.d Comparison whit observations

There exist five tide gauges in the Gulf of California, they are located in La Paz, Bahía de los Angeles, Puerto Peñasco, Guaymas and Topo-

lobampo. They are located in protected areas and are used mainly for harbour work, the local effects are big, but in lack of better information, they were used to compare with computations. Table 1 shows the comparison between observed and computed values. The best correlation was obtained, as expected in La Paz and Topolobampo. Taking in account the paper by Ayala C. y Phleger (1966), there is a phase delay between Topolobampo and the open Gulf of about 15° . This could be the same for La Paz. In the northern part it is found good agreement in phases, but not in amplitudes, as in Bahía de los Angeles and Puerto Peñasco, in both places the phases are reproduced very well, but the amplitudes compare very poorly. One can see a standard deviation of the tide, in the southern part one obtains good agreement with observations and the change of boundary values does not affect the results very much. In the northern part the picture is different, here a small change in the boundaries brings a big change in the results. This might be due to the fact that the northern part of the Gulf has a period of free oscillation similar to the vibration induced by the M_2 wave, also the shallow areas make the water to side up which causes the effect mentioned.

FINAL REMARKS

The method presented here is a good tool to work this kind of computations. It might be that the results could be improved by three different techniques:

a) Taking better boundary values; the values taken in these computations were observed in protected areas where the representation of the real tidewave becomes dubious due to local effects. The best would be to have observations in the actual boundaries.

b) Include in the equations all non-linear terms. Actually equations 4 are a simplification of equations 3. Some of the terms were dropped. These terms are important in some areas, like the region of the islands where sharp bending of the tide occurs, see Brettschneider, (1967).

c) It is also important to compute some of the tidal components

at the same time, the non-linear interaction of the components of different frequencies introduces terms which might give a clearer picture of the energy absorption along the shallow areas.

Nevertheless, a good picture of the propagation of the tide was obtained. The method seems to work in the Gulf of California as it has worked in some other areas, like the North Sea, see Hansen, (1962), The Persian Gulf, Von Trepka, (1967), The Gulf of México, Grijalva, (1971) and also bigger areas like the Atlantic Ocean, Friedrich H. (1967).

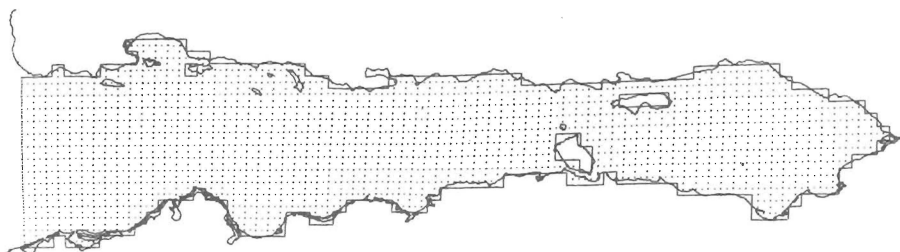


Fig. 1 Gulf of California, The Net Grid (Mercator Projection).

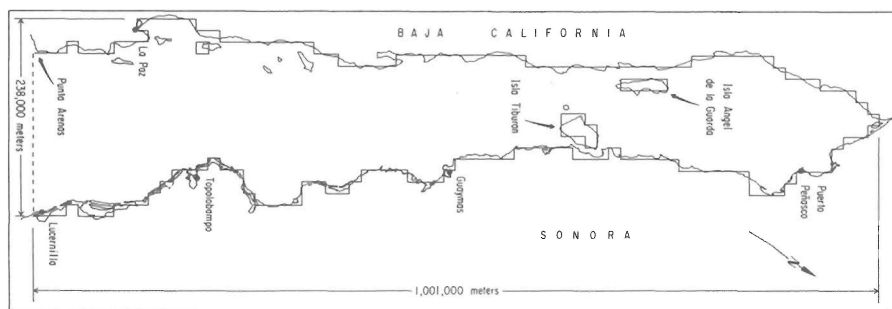


Fig. 2 Reference Chart.

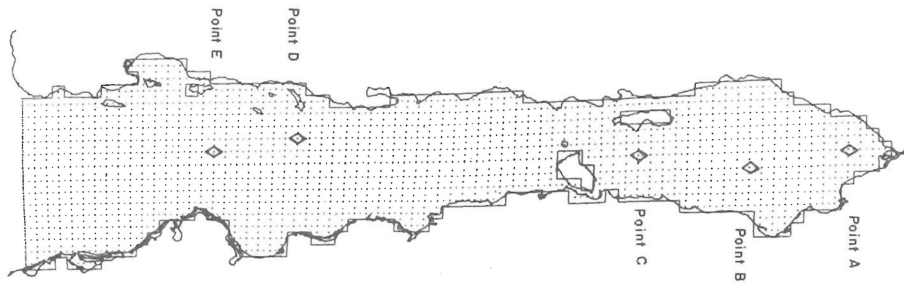


Fig. 3 Gulf of California, Position of Selected Points.

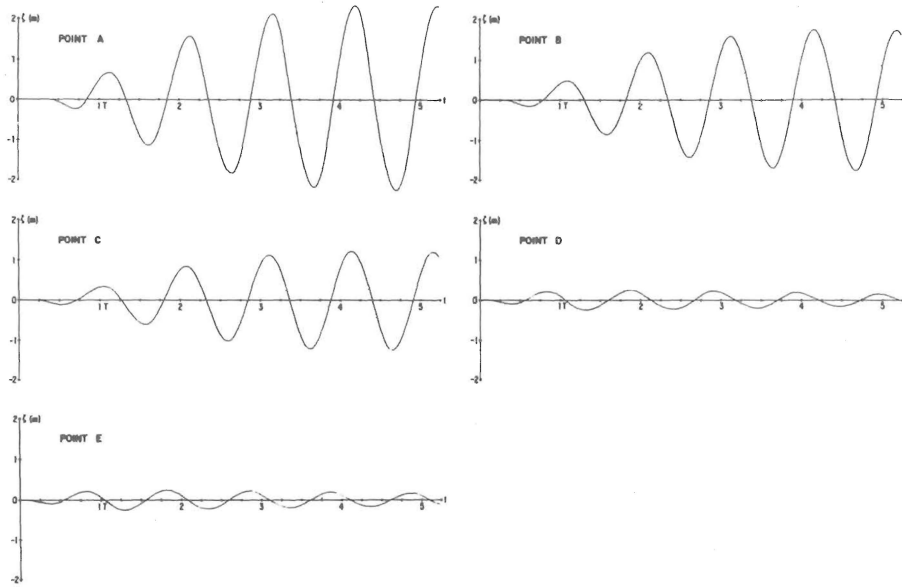


Fig. 4 Process of the tide in 5 selected points.

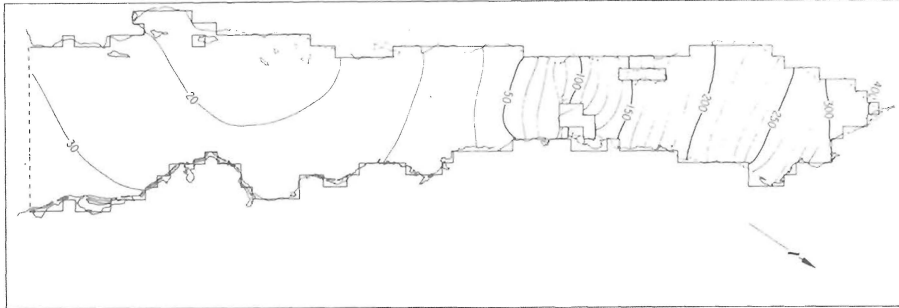
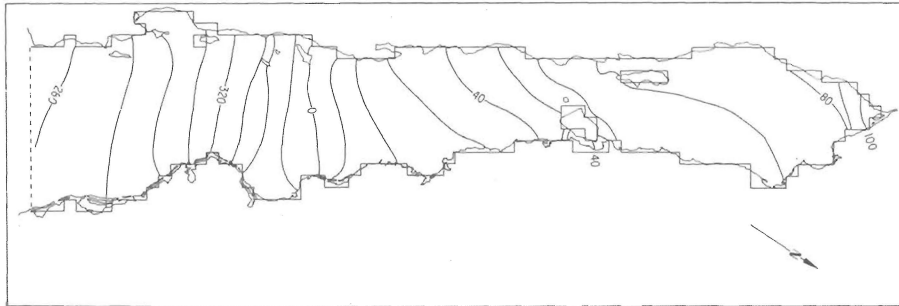


Fig. 5a) First computation, Amplitudes



5b) First computation, Phases (referred to Meridian 105 W of Greenwich)

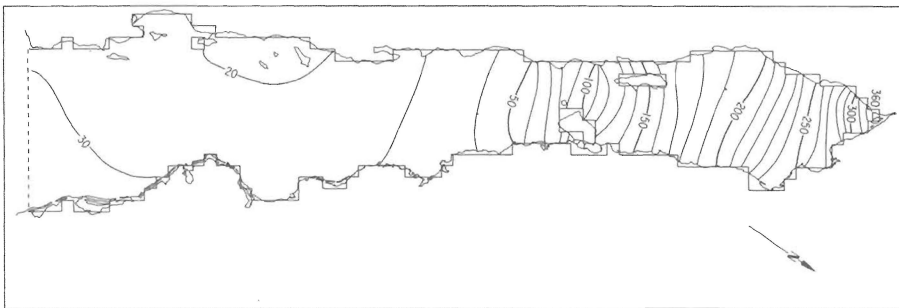
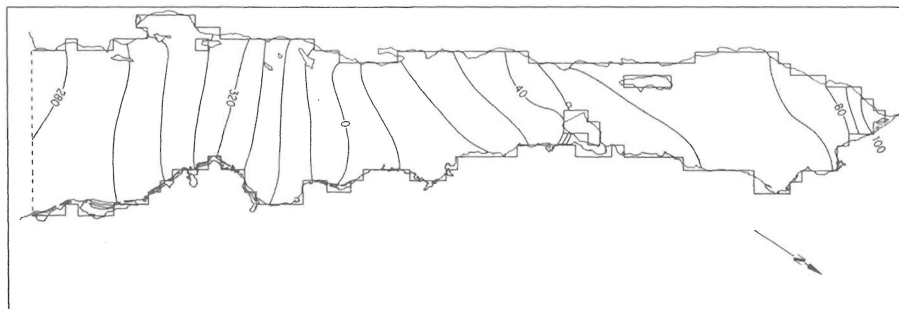


Fig. 6a) Second computation, Amplitudes.



6b) Second computation, Phases.

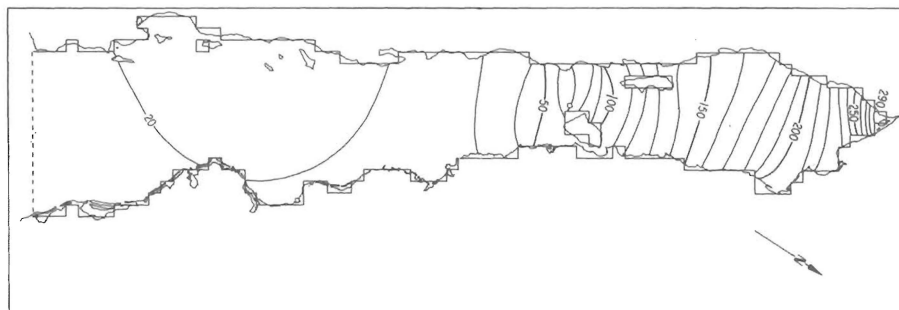
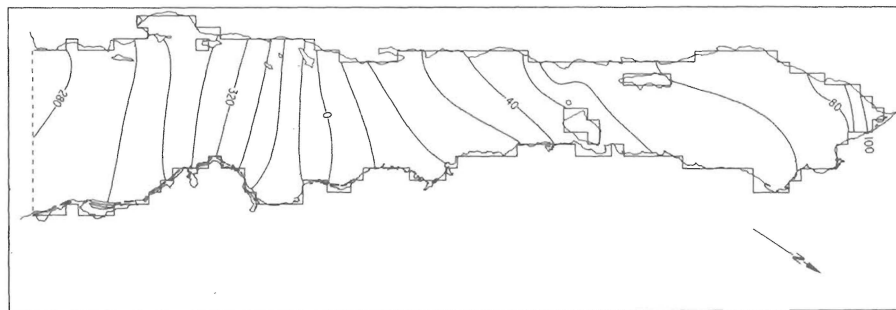


Fig. 7a) Third computation, Amplitudes.



7b) Third computation, Phases.

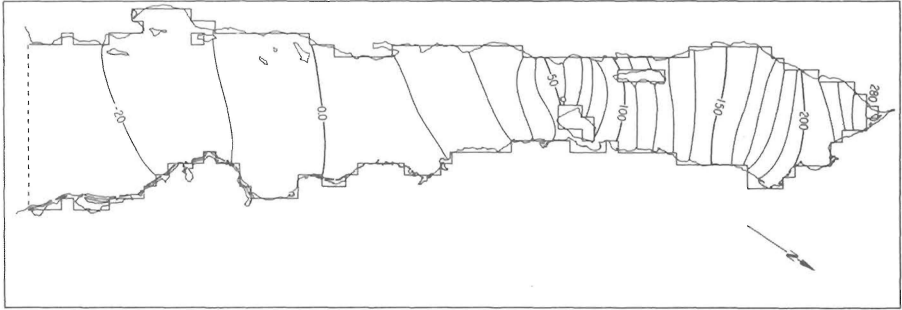
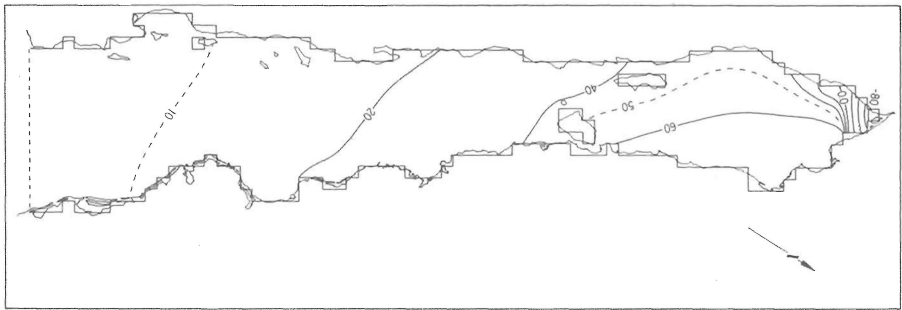


Fig. 8a) Third computation, ζ_1 values (see text 3.3)



8b) Third computation, ζ_2 values (see text 3.3)

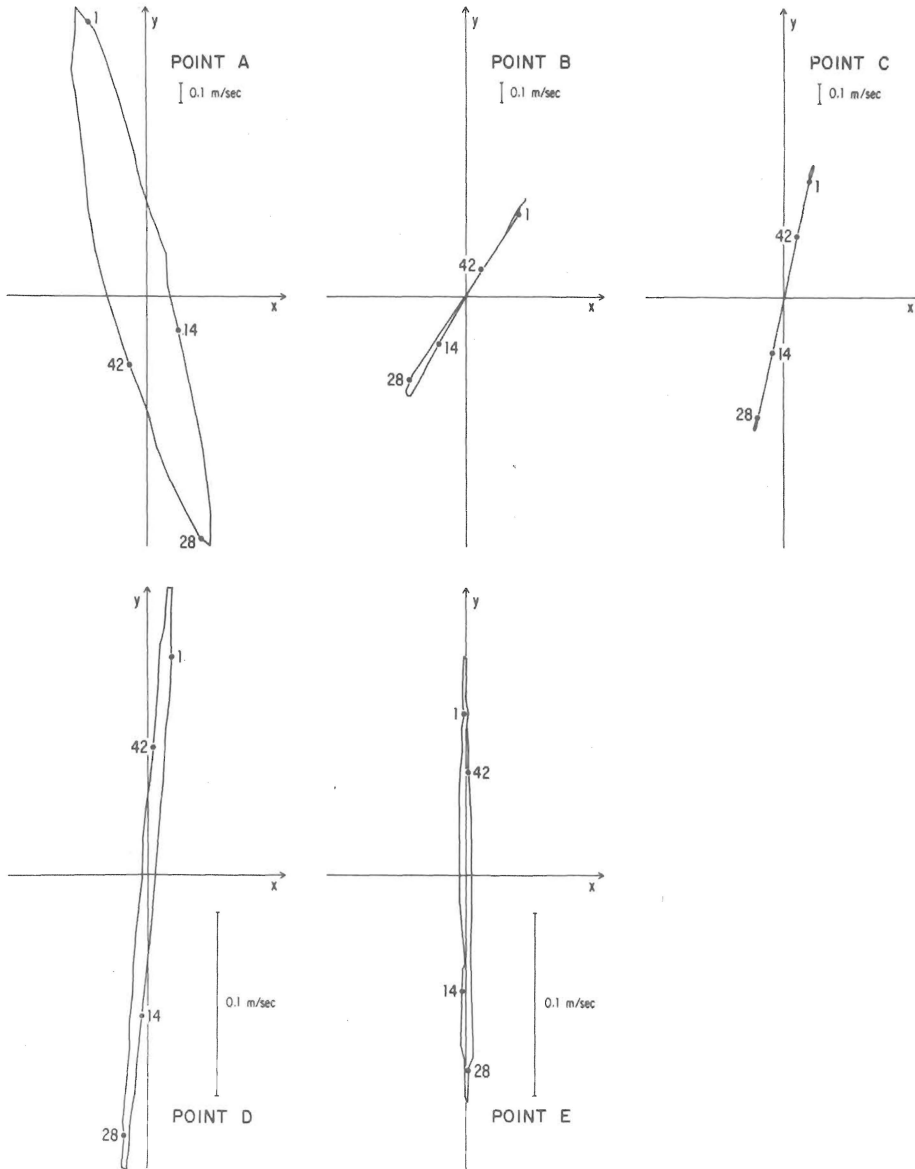


Fig. 9 Tidal currents in selected points.

TABLE 1

<i>Obs Values</i>		COMPUTED		
		<i>First</i>	<i>Second</i>	<i>Third</i>
PUERTO PEÑASCO				
A	1.57	2.80 (185)	2.58 (170)	2.16 (140)
PH	59°	72°	68°	65°
GUAYMAS				
A	0.14	0.35 (250)	0.28 (200)	0.21 (150)
PH	312°	25°	14°	13°
TOPOLOBAMPO				
A	0.30	0.25 (83%)	0.27 (90%)	0.20 (67%)
PH	298°	310°	305°	309°
LA PAZ				
A	0.24	0.20 (83%)	0.22 (92%)	0.17 (70%)
PH	274°	301°	302°	301°
BAHIA DE LOS ANGELES				
A	0.66	1.40	1.35	1.10
PH	62°	72°	62°	66°
YAVAROS				
A	0.221	0.25	0.28	0.22
PH	304°	349°	345°	347°

ACKNOWLEDGMENTS

I wish to express my gratitude to N.S.F. for the Grant No. GA 24523, which made this work possible. Also I would like to thank Drs. C. S. Cox, M. Hendershott, J. Filloux and J. Adem who read the manuscript and made important remarks.

BIBLIOGRAPHY

- A. AYALA C. y F. B. PHLEGER, 1966. Informe Final de la Geología Marina del Area de la Bahía de Topolobampo, Sin. *Instituto de Geología, UNAM.*

- BOWDEN and FAIRBAIRN, 1952. A determination of the frictional forces in a tidal current. *Proc. Roy. Soc. London*, A. 214.
- BRETTSCHEIDER, G., 1967. Anwendung des Hydrodynamisch-Numerischen Verfahrens zur Ermittlung der M_2 Mitschwingungszeit der Nordsee. *Mitt. Inst. Meeresk. Hamburg* Nr. 7.
- DEFANT A. 1962. *Physical Oceanography* Vo. II. *Pergamon Press*.
- J. H. FILLOUX, 1971. Deep-Sea Tide with Optical Readout of Bourdon Tube Rotations. *Nature* Vol. 226, June 6, 1970.
- J. H. FILLOUX, 1971. Deep-Sea Tide Observations from the northeastern Pacific. *Deep-Sea Research*, 1971, Vol. 18, pp. 275-284. *Pergamon Press*.
- GRIJALVA, N., 1964. Numerisch-Hydrodynamische Untersuchungen im Golf von Mexiko. *Dissertation*, Universität Hamburg.
- GRACE, S. F., 1936. Friction in the tidal currents of the Briston Channel. *Mon. Not. Roy. Astr. Soc. Geophys. Suppl.* Vol. 4, No. 2.
- Friction in the tidal currents of the Briston Channel. *Mon. Not. Roy. Astr. Soc. Geophys. Suppl.* Vol. 3, No. 9.
- HANSEN, W., 1952. Gezeiten und Gezeitenströme der halbtägigen Hauptmontide M_2 in der Nordsee. *D. H. Z., Erg. Herft 1*, 1952.
- HANSEN, W., 1956. Theorie zur Errechnung des Wasserstandes und der Stromungen in Randmeeren nebst-Anwendung. *Tellus* 8, Nr. 3.
- HANSEN, W., 1959. Hydrodynamische Methoden in der Ozeanographie. Beiträge zur Physik der Bewegungsvorgänge im Meer. *Geof. Pura e Appl.* 44.
- HANSEN, W., 1962a. Hydrodynamical Methods Applied to Oceanographic Problems. Proc. of the Symposium on Mathematical-Hydrodynamical Methods of Physical Oceanography. *Mitt. Inst. Meersk. Hamburg* Nr. 1.
- HANSEN, W., 1962b. Tides – The Sea, Ideas and Observations on Progress in the Study of the Sea. Vol. 1. *M. N. Hill. Intersc. Publ. Inc.*, New York.
- M. C. HENDERSHOTT and A. SPERANZA, 1971. Co-oscillation tides in long narrow bays; the Taylor problem revisited. *Deep-Sea Research*, 1971, Vol. 18 pp. 959-980. *Pergamon Press*.
- ISAAC, J., REID, J., SCHICK, G. & SCHWARTZLOSE, R., 1966. Tidal measurements off the Gulf of California. *J. Geophys. Res.*, 1971, 4297.
- LAMB H. Sir., 1962. *Hydrodynamics*. *Cambridge University Press*.
- LARSEN, J., 1966. Electric and Magnetic Fields Induced by Deep Sea Tides. *J. Geophys. Res.*, 71, 4441.
- KRUMEL O., 1911. *Handbuch der Ozeanographie* 2 pp. 766 (2n eed) Stuttgart: J. Engelhorn.
- TAYLOR, G. I., 1919. Tidal Friction in the Irish Sea. *Phil. Trans. Roy. Soc.*, London, A. 220.
- TAYLOR, G.I., 1919. Tidal oscillations in gulfs and rectangular basins. *Proc. London. Math. Soc.*, 2, 20.